

of  $(C_5H_5)_2Ln$  units is favorable<sup>2,3</sup> and can be modified to some extent. Extensions to central  $S^{2-}$  and  $N^{3-}$  ligands are suggested by this result.

The existence of the inverse sandwich counteraction  $\{[(THF)_3Na]_2(\mu-\eta^5:\eta^5-C_5H_5)\}^+$  in **2** shows that the cyclopentadienyl ion can be more than an innocent contaminant in these reaction systems. In conjunction with alkali metals, it can provide a counteraction of substantial size. Given that ligand disproportionation can occur and cyclopentadienyl ligands can be displaced in f element complexes,<sup>68,71</sup> the possible presence of  $[M_2(\mu-C_5R_5)]^+$  cations must be considered in cyclopentadienyl systems containing alkali-metal ions.

The pentametallic structure of **3** has turned out to be a common form of self-assembly in alkoxide systems involving yttrium, lanthanide, and metals of similar sizes.<sup>15-18</sup> Comparison of these structures with **3** (Table VII) indicates that the combination of  $C_5H_5$  and OMe ligand is sterically equivalent to the bulk provided by isopropoxide ligands.

In the sense that the square pyramid is comprised of four triangles, each of which contains a multiply-bridging ligand above and below the plane, this structure is also relatable to the trimetallic yttrium *tert*-butoxide complexes such as  $Y_3(OCMe_3)_8Cl(THF)_2$  and  $[Y_4(OR)_{10}Cl_2O]^{2-}$  which contain the basic unit  $Ln_3(\mu-OR)_3(\mu_3-Z)_2$  ( $Z = OR$ , halide, or oxide).<sup>2</sup> In the case of **3**, the triply-bridging ligands are a methoxide on one side of the  $Y_3$  triangle and the oxide on the other side, which since it is shared by all of the triangles is a  $\mu_5$ -ligand. As in  $[Y_4(OR)_{10}Cl_2O]^{2-}$ , the edges of the triangles which are fused do not have the  $\mu_2$ -alkoxide ligand, and hence **3** has only four  $\mu_2$ -OMe ligands along the base. In this comparison, the  $C_5H_5$ /OMe ligand combination is functioning as the equivalent of the *tert*-butoxide ligand. If one considers the trimetallic bis(cyclopentadienyl)yttrium alkoxide complexes such as **2** and  $\{[(C_5H_5)_2Y(\mu-OMe)]_3(\mu-H)\}^{3-}$ <sup>37</sup> as additional variations on the basic  $Ln_3(\mu-OR)_3(\mu_3-Z)_2$

unit, one can see a continuous series of structural possibilities based on triangular units with various combinations of alkoxide and cyclopentadienyl ligands.

### Conclusion

The reaction of methoxide ion with  $(C_5H_5)_2YCl(THF)$  has produced an unexpected amount of information on the chemistry of cyclopentadienyl yttrium alkoxides. These reactions can be much more complicated than anticipated and demonstrate how carefully reaction details must be controlled in some lanthanide-based systems. A variety of reaction pathways are readily accessible, and small changes in the concentration of reagents can alter the course of the reaction in a major way. In addition, the preparation of the starting materials and product isolation procedures can have profound effects on the course of the reaction. This study also shows that oxide-containing products can be obtained in the presence of water-scavenging ligands such as  $C_5H_5^-$  in reactions which form byproducts consistent with methoxide to oxide conversions. The variations observed in this reaction chemistry along with the considerable structural variety which appears to be accessible through bridged trimetallic complexes of these metals indicate that, to do future mechanistic studies of clean reaction systems, the components must be chosen very carefully.

**Acknowledgment.** For support of this research, we thank the Division of Chemical Sciences of the Office of Basic Energy Sciences of the Department of Energy. Funds for the purchase of the Siemens R3m/V diffractometer system were made available from the National Science Foundation under Grant CHE-85-14495.

**Supplementary Material Available:** Tables of bond distances and angles, thermal parameters, crystal data, details of intensity data collection and structure refinement, atomic positional parameters, temperature factors, and H atom coordinates and displacement coefficients, ball and stick diagrams, ORTEP diagrams, and textual presentation of X-ray data collection and structure determination and refinement (43 pages); tables of structure factor amplitudes (27 pages). Ordering information is given on any current masthead page.

(71) Evans, W. J.; Boyle, T. J. Unpublished results.

Contribution from the Departamento de Química Inorgánica, Facultad de Ciencias, Universidad de Valladolid, 47011 Valladolid, Spain, Departamento de Química Inorgánica, Colegio Universitario de Burgos, 09002 Burgos, Spain, and Laboratoire de Chimie des Métaux de Transition, UA-CNRS 419, Université Pierre et Marie Curie, 4 Place Jussieu, 72252 Paris Cedex 05, France

## Double Oxidative Carbon-Carbon Coupling of a Dimeric Orthopalladated Amido Complex Leading to Redox-Active Tetrapalladia Units $[Pd_4]^{n+}$ ( $n = 0-4$ )

Pablo Espinet,<sup>\*,†</sup> María Y. Alonso,<sup>‡</sup> Gabriel Garcia-Herbosa,<sup>‡</sup> José M. Ramos,<sup>‡</sup> Y. Jeannin,<sup>§</sup> and M. Philoche-Levisalles<sup>§</sup>

Received October 16, 1991

Chemical or electrochemical oxidation of the chiral orthometalated amido dimeric complex  $[Pd-o-C_6H_4-C(Me)=N-NPh]L_2$  ( $L = P(OMe)_3$ ) leads to double carbon-carbon coupling on the para carbons of the phenyl groups, giving pure diastereomeric tetrapalladia units  $[Pd_4]^{n+}$  ( $n = 0-4$ ) related by fully reversible mono-electronic electron transfers. The species  $[Pd_4]^{4+}$  undergoes splitting with  $Cl^-$ , giving dimeric units  $[Pd_2]$  where a 4,4'-biphenylene quinone diimine is trapped and stabilized between two palladia atoms; reduction with  $CoCp_2$  affords a mixture of both possible diastereomers of  $[Pd_4]^0$ . Near-infrared absorptions have been observed for paramagnetic  $[Pd_4]^{3+}$ , which can be regarded as a "mixed oxidation state" compound. The structure of  $[Pd-o-C_6H_4-C(Me)=N-NPh-p-NO_2]L_2$  ( $L = P(OMe)_3$ ), where coupling is precluded by  $NO_2$  groups, was determined crystallographically [space group  $P\bar{1}$  (triclinic),  $a = 10.901(16)$  Å,  $b = 13.744(9)$  Å,  $c = 14.242(5)$  Å,  $\alpha = 73.41(4)^\circ$ ,  $\beta = 87.61(6)^\circ$ ,  $\gamma = 81.00(8)^\circ$ ,  $V = 2020(5)$  Å<sup>3</sup>,  $Z = 2$ ].

### Introduction

Mixed-valence polynuclear complexes are of current interest,<sup>1</sup> as they exhibit unusual structural, bonding, reactivity, spectroscopic, and magnetic properties<sup>2</sup> which can find applications in areas such as the study of electron-transfer processes<sup>3</sup> and the design of molecular electronics.<sup>4</sup>

We have previously prepared and described<sup>5</sup> binuclear orthometalated complexes of palladium(II) which could be used as precursors to prepare potentially mixed-valence compounds. The

<sup>†</sup> Universidad de Valladolid.

<sup>‡</sup> Colegio Universitario de Burgos.

<sup>§</sup> Université Pierre et Marie Curie.

(1) For recent literature on "mixed valence" compounds see for instance: Haga, M. A.; Bond, A. M. *Inorg. Chem.* **1991**, *30*, 475 and references therein.

(2) Creutz, C. *Prog. Inorg. Chem.* **1983**, *30*, 1.

(3) Taube, H. *Angew. Chem., Int. Ed. Engl.* **1984**, *23*, 329.

(4) Mikkelsen, K. V.; Ratner, M. A. *Chem. Rev.* **1987**, *87*, 113.

(5) Espinet, P.; Garcia-Herbosa, G.; Herrero, F. J.; Jeannin, Y.; Philoche-Levisalles, M. *Inorg. Chem.* **1989**, *28*, 4207.

presence of unusual Pd–N amido bonds in these complexes adds further interest on the basis of the reactivity shown by amides of the platinum group metals.<sup>6</sup>

Formation of carbon–carbon bonds is quite common in electron-transfer reactions,<sup>7–10</sup> sometimes leading to polymers with special electrical properties;<sup>11–13</sup> chemical oxidative C–C coupling in amido complexes of platinum has been described,<sup>14,15</sup> and we have shown<sup>16</sup> that the use of electrochemical techniques to characterize the processes allows a better understanding of the nature of the reaction and the products formed. Here we describe the double oxidative coupling of a binuclear orthometalated Pd(II) amido complex, leading to a family of tetranuclear compounds (Scheme I) which are represented in the following as  $[\text{Pd}_4]^{n+}$ , where  $n = 0–4$ . The chemical and electrochemical behavior of these complexes is presented and discussed below.

## Experimental Section

**Synthesis.** Dimeric complexes  $[\text{Pd}-\sigma\text{-C}_6\text{H}_4-\text{C}(\text{Me})=\text{N}-\text{NPh}-p\text{-X})\text{L}]_2$  [L = P(OMe)<sub>3</sub>, X = H, I; L = P(OMe)<sub>3</sub>, X = NO<sub>2</sub>, 2; L = 4-methylpyridine, X = H, 1a; L = 4-methylpyridine, X = NO<sub>2</sub>, 2a],<sup>5</sup> cobaltocene,<sup>17</sup> and  $[\text{Cp}_2\text{Fe}][\text{PF}_6]$ <sup>18</sup> were prepared according to published methods (for the synthesis of 2 and 2a acetophenone (*p*-nitrophenyl)hydrazine was used instead of acetophenone phenylhydrazine). Solvents were dried and distilled prior to use, and the reactions were carried out under nitrogen or argon by using standard Schlenk techniques.

**$[\text{Pd}_4][\text{PF}_6]_2$  ( $3^{2+}$ ).** To a solution of 1 (2 g, 2.28 mmol) in 50 mL of dichloromethane was added 0.76 g (2.28 mmol) of  $[\text{Cp}_2\text{Fe}][\text{PF}_6]$ . After stirring for 15 h, filtration afforded a first crop (0.23 g) of a greenish-black solid. To the solution was added 25 mL of toluene. Concentration to approximately two-thirds of the initial volume afforded a second crop (0.32 g), which was collected by filtration and dried. Yield: 24%. Anal. Calcd for  $\text{C}_{68}\text{H}_{80}\text{N}_8\text{O}_{12}\text{P}_8\text{F}_{12}\text{Pd}_4$ : C, 40.02; H, 3.95; N, 5.49. Found: C, 39.95; H, 3.81; N, 5.44.

**$[\text{Pd}_4][\text{PF}_6]_4$  ( $3^{4+}$ ).** To a solution of  $3^{2+}$  (200 mg, 0.1 mmol) in 30 mL of dichloromethane was added 67 mg (0.2 mmol) of  $[\text{Cp}_2\text{Fe}][\text{PF}_6]$ . Stirring for 10 min and addition of *n*-hexane to induce precipitation afforded the complex as a bluish-black solid in nearly quantitative yield. Anal. Calcd for  $\text{C}_{68}\text{H}_{80}\text{N}_8\text{O}_{12}\text{P}_8\text{F}_{24}\text{Pd}_4$ : C, 35.04; H, 3.46; N, 4.81. Found: C, 34.84; H, 3.35; N, 4.65.

**$[\text{Pd}_4][\text{PF}_6]_3$  ( $3^{3+}$ ).** **Method a.** To a solution of  $3^{2+}$  (100 mg, 0.05 mmol) of 20 mL of dichloromethane was added 17 mg (0.05 mmol) of  $[\text{Cp}_2\text{Fe}][\text{PF}_6]$ . Stirring for 10 min and addition of *n*-hexane (10 mL) afforded the complex as a brownish-black solid in nearly quantitative yield.

**Method b.** To a solution of  $3^{2+}$  (50 mg, 0.024 mmole) in 20 mL of dichloromethane was added 56 mg (0.024 mmol) of  $3^{4+}$ . Stirring for 5 min and addition of hexane (10 mL) yielded the complex quantitatively. Anal. Calcd for  $\text{C}_{68}\text{H}_{80}\text{N}_8\text{O}_{12}\text{P}_7\text{F}_{18}\text{Pd}_4$ : C, 37.37; H, 3.69; N, 5.13. Found: C, 37.02; H, 3.52; N, 5.04.

**$[\text{Pd}_4]^0$  (3).** To a solution of  $3^{2+}$  (200 mg, 0.1 mmol) in 30 mL of dichloromethane was added 38 mg (0.2 mmol) of  $\text{CoCp}_2$ . The solution turned dark green, and the solvent was pumped off. The residue was treated with 20 mL of toluene, the solution was filtered, and *n*-hexane (20 mL) was added. Concentration under vacuum gave the complex as a dark green powder. Yield: 100 mg, 65%. Anal. Calcd for

**Table I.** Crystallographic Data for Complex 2

|                  |  |  |               |
|------------------|--|--|---------------|
| chemical formula | $\text{Pd}_2\text{P}_2\text{O}_{10}\text{N}_6\text{C}_{34}\text{H}_{40}$ | $V, \text{Å}^3$                        | 2020 (5)      |
| fw               | 967.47   | Z                                      | 2             |
| space group      | $P\bar{1}$   | $T, ^\circ\text{C}$                    | 20            |
| a, Å             | 10.901 (16)  | radiation                              | Mo K $\alpha$ |
| b, Å             | 13.744 (9)   | $\rho_{\text{calc}}, \text{g cm}^{-3}$ | 1.59          |
| c, Å             | 14.242 (5)   | $\mu, \text{cm}^{-1}$                  | 10.1          |
| $\alpha$ , deg   | 73.41 (4)  | $R(F)^a$                               | 0.056         |
| $\beta$ , deg    | 87.61 (6)  | $R_w(F)^a$                             | 0.064         |
| $\gamma$ , deg   | 81.00 (8)  |  |               |

<sup>a</sup>  $R(F) = \sum |F_o| - |F_c| / \sum |F_o|$ ;  $R_w(F) = [\sum w(|F_o| - |F_c|)^2 / \sum w|F_o|^2]^{1/2}$ ;  $w = w' [1 - \{(F_o - F_c) / 6\sigma(F_o)\}^2]$ , where  $w' = 1 / \sum_{j=1,3,5,7} A_j T_j(X)$  with coefficients  $A = 2.795, 0.059$ , and 1.945 for the Chebyshev polynomial  $T_j(X)$  with  $X = F_o / F_o(\text{max})$ .

$\text{C}_{68}\text{H}_{80}\text{N}_8\text{O}_{12}\text{P}_8\text{Pd}_4$ : C, 46.65; H, 4.60; N, 6.40. Found: C, 46.52; H, 4.54; N, 6.38. <sup>1</sup>H NMR ( $\delta$ ,  $\text{C}_6\text{D}_6$ ):  $\text{CH}_3$ , 2.32 (s, 12 H);  $\text{OCH}_3$ , 3.33 (d, 36 H, <sup>3</sup> $J_{\text{P-H}} = 13$  Hz); phenyl rings, 6.44, 7.00–7.50, 7.99 (m, 32 H). <sup>31</sup>P NMR (at 121.5 MHz,  $\delta$ ,  $\text{C}_6\text{D}_6$ , ref 85%  $\text{H}_3\text{PO}_4$ ): 130.77.

**Complex 4.** To a dark green solution of 3 (50 mg, 0.03 mmol) in 10 mL of dichloromethane was added hydrochloric acid (0.6 mL of a 0.1 M solution, 0.06 mmol). Vigorous stirring for 1 min turned the solution yellow. Addition of *n*-hexane (10 mL) and concentration to a small volume afforded a yellow solid which was recrystallized from dichloromethane/*n*-hexane and dried under vacuum. Yield: 42 mg, 75%. Anal. Calcd for  $\text{C}_{38}\text{H}_{42}\text{N}_4\text{O}_6\text{P}_2\text{Cl}_2\text{Pd}_2$ : C, 43.06; H, 4.46; N, 5.91. Found: C, 42.95; H, 4.28; N, 5.80. <sup>1</sup>H NMR ( $\delta$ ,  $\text{CDCl}_3$ ):  $\text{CH}_3$ , 2.35 (s, 6 H);  $\text{OCH}_3$ , 3.78 (d, 18 H, <sup>3</sup> $J_{\text{P-H}} = 13$  Hz); phenyl rings, 6.75, 7.14, 7.39 (m, 16 H).

**Complex 4a.** This compound was prepared as for 4 but using concentrated acetic acid (0.06 mmol) instead of hydrochloric acid. Yield: 45 mg, 80%. Anal. Calcd for  $\text{C}_{38}\text{H}_{48}\text{N}_4\text{O}_{10}\text{P}_2\text{Pd}_2$ : C, 45.84; H, 4.86; N, 5.63. Found: C, 45.58; H, 4.78; N, 5.52. <sup>1</sup>H NMR ( $\delta$ ,  $\text{CDCl}_3$ ):  $\text{CH}_3$ , 1.93 (s, 6 H);  $\text{CH}_3$ , 2.35 (s, 6 H);  $\text{OCH}_3$ , 3.78 (d, 18 H, <sup>3</sup> $J_{\text{P-H}} = 13$  Hz); phenyl rings, 6.75, 7.14, 7.39 (m, 16 H).

**Complex 6.** To a solution of  $3^{4+}$  (100 mg, 0.04 mmol) in 20 mL of dichloromethane was added 39 mg (0.17 mmol) of benzyltriethylammonium chloride. After stirring for 30 min, the solvent was removed in vacuum. Toluene (20 mL) was added to the residue and the purple solution was poured into *n*-hexane (50 mL), giving a black precipitate. Yield: 63 mg, 83%. Anal. Calcd for  $\text{C}_{34}\text{H}_{40}\text{N}_4\text{O}_6\text{P}_2\text{Cl}_2\text{Pd}_2$ : C, 43.15; H, 4.26; N, 5.92. Found: C, 42.85; H, 4.18; N, 5.74. <sup>1</sup>H NMR ( $\delta$ ,  $\text{CDCl}_3$ ):  $\text{CH}_3$ , 2.32 (s, 6 H);  $\text{OCH}_3$ , 3.79 (d, 18 H, <sup>3</sup> $J_{\text{P-H}} = 13$  Hz); phenyl rings, 7.09–7.71 (m, 16 H).

**$[\text{Pd}_4]^0$  (Isomeric Mixture of 3).** To a solution of 6 (100 mg, 0.1 mmol) in 10 mL of dichloromethane was added 38 mg (0.2 mmol) of  $\text{CoCp}_2$ . The purple solution turned dark green, and the solvent was removed in vacuum. The residue was treated with toluene (20 mL) and filtered. Addition of *n*-hexane (20 mL) and concentration afforded a 1:1 isomeric mixture (meso + rac) of the complex. Yield: 72 mg, 78%. Anal. Calcd for  $\text{C}_{68}\text{H}_{80}\text{N}_8\text{O}_{12}\text{P}_8\text{Pd}_4$ : C, 46.65; H, 4.60; N, 6.40. Found: C, 46.48; H, 4.50; N, 6.30. <sup>1</sup>H NMR ( $\delta$ ,  $\text{C}_6\text{D}_6$ ):  $\text{CH}_3$ , 2.32 (s, 12 H);  $\text{OCH}_3$ , 3.33 (d, 18 H, <sup>3</sup> $J_{\text{P-H}} = 13$  Hz), 3.34 (d, 18 H, <sup>3</sup> $J_{\text{P-H}} = 13$  Hz); phenyl rings, 6.44, 7.00–7.50, 7.99 (m, 32 H). <sup>31</sup>P NMR (at 121.5 MHz,  $\delta$ ,  $\text{C}_6\text{D}_6$ , ref 85%  $\text{H}_3\text{PO}_4$ ): 130.8, 129.8.

**Electrochemistry.** Cyclic voltammetry (CV), controlled-potential electrolysis (CPE), and rotating electrode (RE) experiments were carried out using an AMEL 551 potentiostat–amperostat and a Tacussel GSTP signal generator in conjunction with a three-electrode cell under experimental conditions described elsewhere.<sup>16</sup>

**EPR and NMR Measurements.** X-Band ESR spectra were recorded on a Varian Associates 4502/15 instrument. <sup>1</sup>H, <sup>13</sup>C, and <sup>31</sup>P NMR spectra were recorded on Bruker spectrometer AC-80 (80 MHz for proton) or AC-300 (300 MHz for proton).

**X-ray Data and Structure Refinement.** Crystals of 2 were grown by the slow diffusion of *n*-hexane into a solution of the complex in dichloromethane. The crystallographic measurements were carried out on a Philips PW 1100 diffractometer,  $\omega$ – $2\theta$  mode, with scan width 1.2 + 0.34 tan  $\theta$ , graphite monochromator, Mo K $\alpha$  radiation, room temperature. The recording  $\theta$  range was 1–25°. A total of 6488 independent reflections was observed. Two standard reflections were measured every 2 h, with no deviation observed. Absorption correction was made by an empirical method based on the  $\psi$ -scan of one reflection (min–max correction factor 1.00–1.20),  $\mu = 10.1 \text{ cm}^{-1}$ . The structure was solved by the Patterson method and subsequent Fourier maps. Least-squares refinements were made in two blocks (490 parameters). Some hydrogen atoms were found on a difference map; others were geometrically positioned. They were not refined and were given an overall isotropic thermal parameter. Atoms were corrected from anomalous dispersion, and a

- Fryzuk, M. D.; Montgomery, C. D. *Coord. Chem. Rev.* **1989**, *95*, 1.
- Adams, H.; Bailey, N. A.; Willett, D. G.; Winter, M. J. *J. Organomet. Chem.* **1987**, *333*, 61.
- Aggarwal, R. P.; Connelly, N. G.; Dunne, B. J.; Gilbert, M.; Orpen, A. G. *J. Chem. Soc., Dalton Trans.* **1991**, 1.
- Filippou, A. C.; Grünleitner, W. *J. Organomet. Chem.* **1990**, *393*, C10.
- Klein, H. F.; Beck-Menetsberger, H.; Reitzel, L.; Rodenhäuser, B.; Cordier, G. *Chem. Ber.* **1989**, *122*, 43.
- Casbore-Miceli, G.; Beggiato, G. S.; Emmi, S. S.; Geri, A. *J. Appl. Electrochem.* **1988**, *18*, 885.
- Casbore-Miceli, G.; Beggiato, G.; Daolio, S.; Marco, P. G. D.; Emmi, S. S.; Giro, G. *J. Appl. Electrochem.* **1987**, *17*, 1111.
- Yue, J.; Epstein, A. J. *J. Am. Chem. Soc.* **1990**, *112*, 2800.
- O'Sullivan, R. D.; Parkins, A. W.; Alcock, N. W. *J. Chem. Soc. Dalton Trans.* **1986**, 571.
- Alcock, N. W.; O'Sullivan, R. D.; Parkins, A. W. *J. Chem. Soc., Chem. Commun.* **1980**, 1286.
- Espinete, P.; Garcia-Herbosa, G.; Ramos, J. M. *J. Chem. Soc., Dalton Trans.* **1990**, 2931.
- King, R. B. *Organometallic Syntheses*; Eisch, J. J., King, R. B., Eds.; Academic Press: New York, 1965; pp 70.
- Smart, J. C.; Pinsky, B. L. *J. Am. Chem. Soc.* **1980**, *102*, 1009.

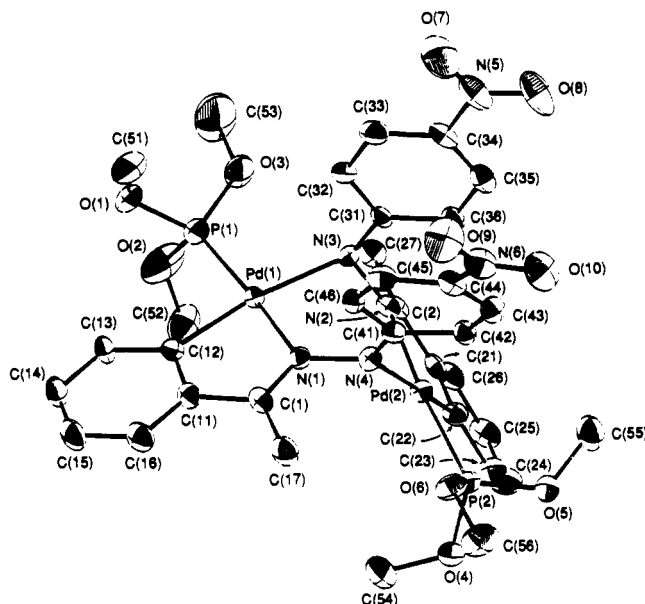
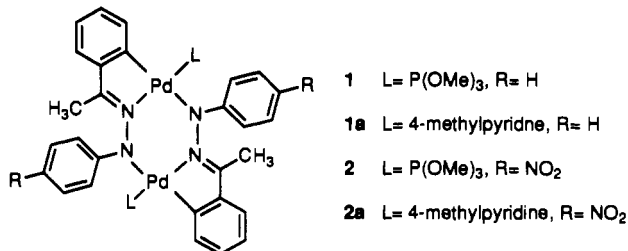


Figure 1. ORTEP view of the structure of **2** with the numbering scheme.

secondary extinction correction was applied. Refinements converged at  $R = 5.64\%$ ,  $R_w = 6.36\%$ . The final positional and thermal parameters are shown in Table II; distances and angles are given in Table III. Figure 1 shows a perspective view of the molecule with the numbering scheme.

### Results

CV (cyclic voltammetry) experiments (Table IV) show that the binuclear complexes **1**, **1a** (dark blue), **2**, and **2a** (red) undergo



two one-electron oxidative transitions which are reversible for **2** and **2a** and irreversible for **1** and **1a**, indicating that a chemical process follows oxidation in the latter two.

In order to discount structural differences in these dimers as the reason for the different color and electrochemical behavior, an X-ray structural determination of complex **2** was undertaken. The structure and atom-numbering scheme of complex **2** are shown in Figure 1; it is very similar to that of **1** previously studied.<sup>5</sup>

The six-membered dipalladiacycle Pd(1)-N(1)-N(4)-Pd(2)-N(2)-N(3) has a roof shape with a hinge through N(3)-N(4) and a dihedral angle of 117.4°. The dihedral angles N(4)-N(1)-Pd(1)-N(3) and N(3)-N(2)-Pd(2)-N(4) are respectively +2.2 and -1.6°. A mean square plane calculation including Pd(1)-P(1)-C(1)-C(11)-N(1)-N(3)-N(4) and the phenyl ring C(11) to C(16) shows that the largest deviation occurs at N(3) with 0.23 Å, and for Pd(2) and equivalent atoms the largest deviation is 0.11 Å for N(1). The equivalent angles around N(3) and N(4) are unexpectedly different, a feature also found in the structure of **1**.<sup>5</sup> The phenyl ring C(31) to C(35) is nearly parallel, making an angle of 18°. In summary, no significant structural differences are found between **1** and **2**.

Attempts at chemical oxidation of **2** or **2a** with [(*p*-Br-C<sub>6</sub>H<sub>4</sub>)<sub>3</sub>N]<sup>+</sup> (prepared "in situ" with [NO]BF<sub>4</sub> and tris(*p*-bromophenyl)amine) in CH<sub>2</sub>Cl<sub>2</sub> did not afford oxidized products, and the starting complexes were recovered unchanged from the solutions.

On the other hand, chemical oxidation of **1** with [Cp<sub>2</sub>Fe]PF<sub>6</sub> in CH<sub>2</sub>Cl<sub>2</sub>, molar ratio 1:1, afforded complex 3<sup>2+</sup>, which gives the cyclic voltammogram shown in Figure 2. The RE (rotating

Table II. Positional and Thermal Parameters (with Esd's in Parentheses) for C<sub>34</sub>H<sub>40</sub>N<sub>6</sub>O<sub>10</sub>P<sub>2</sub>Pd<sub>2</sub>

| atom  | <i>x/a</i>  | <i>y/b</i>  | <i>z/c</i>  | <i>U</i> <sub>eq</sub> , Å <sup>2</sup> |
|-------|-------------|-------------|-------------|---|
| Pd(1) | 0.29220 (5) | 0.45849 (4) | 0.19784 (3) | 0.0345                                  |
| Pd(2) | 0.37891 (5) | 0.17308 (4) | 0.22370 (4) | 0.0354                                  |
| P(1)  | 0.3694 (2)  | 0.5831 (1)  | 0.2345 (1)  | 0.0402                                  |
| P(2)  | 0.3385 (2)  | 0.0646 (2)  | 0.1445 (2)  | 0.0518                                  |
| N(1)  | 0.2035 (5)  | 0.3577 (4)  | 0.1502 (4)  | 0.0362                                  |
| N(2)  | 0.4294 (5)  | 0.2615 (4)  | 0.3091 (4)  | 0.0361                                  |
| N(3)  | 0.3482 (5)  | 0.3434 (4)  | 0.3297 (4)  | 0.0384                                  |
| N(4)  | 0.1972 (5)  | 0.2570 (4)  | 0.2063 (4)  | 0.0362                                  |
| N(5)  | 0.1798 (7)  | 0.3234 (6)  | 0.7099 (5)  | 0.0640                                  |
| N(6)  | -0.0967 (7) | 0.2098 (7)  | 0.5423 (6)  | 0.0697                                  |
| O(1)  | 0.2781 (5)  | 0.6852 (4)  | 0.2297 (5)  | 0.0570                                  |
| O(2)  | 0.4746 (5)  | 0.6340 (4)  | 0.1677 (4)  | 0.0549                                  |
| O(3)  | 0.4278 (5)  | 0.5445 (4)  | 0.3413 (4)  | 0.0518                                  |
| O(4)  | 0.396 (1)   | 0.0706 (6)  | 0.0413 (6)  | 0.0902                                  |
| O(5)  | 0.3879 (6)  | -0.0526 (4) | 0.1894 (6)  | 0.0674                                  |
| O(6)  | 0.1965 (6)  | 0.0691 (5)  | 0.1343 (7)  | 0.0739                                  |
| O(7)  | 0.1175 (7)  | 0.4010 (6)  | 0.7233 (5)  | 0.0779                                  |
| O(8)  | 0.2115 (9)  | 0.2461 (6)  | 0.7777 (5)  | 0.0909                                  |
| O(9)  | -0.1710 (7) | 0.2837 (7)  | 0.5522 (5)  | 0.0862                                  |
| O(10) | -0.0838 (9) | 0.1249 (7)  | 0.6055 (6)  | 0.1035                                  |
| C(1)  | 0.1685 (6)  | 0.3877 (5)  | 0.0594 (5)  | 0.0353                                  |
| C(2)  | 0.5441 (6)  | 0.2437 (5)  | 0.3353 (5)  | 0.0403                                  |
| C(11) | 0.1886 (5)  | 0.4926 (5)  | 0.0078 (4)  | 0.0339                                  |
| C(12) | 0.2449 (6)  | 0.5454 (5)  | 0.0612 (5)  | 0.0423                                  |
| C(13) | 0.2660 (8)  | 0.6462 (6)  | 0.0120 (5)  | 0.0533                                  |
| C(14) | 0.2341 (8)  | 0.6908 (7)  | -0.0864 (6) | 0.0604                                  |
| C(15) | 0.1791 (7)  | 0.6374 (7)  | -0.1373 (5) | 0.0532                                  |
| C(16) | 0.1558 (6)  | 0.5392 (6)  | -0.0905 (5) | 0.0435                                  |
| C(17) | 0.1110 (7)  | 0.3228 (6)  | 0.0116 (5)  | 0.0493                                  |
| C(21) | 0.6196 (7)  | 0.1592 (5)  | 0.3039 (5)  | 0.0414                                  |
| C(22) | 0.5600 (6)  | 0.1127 (5)  | 0.2465 (5)  | 0.0428                                  |
| C(23) | 0.6345 (7)  | 0.0387 (6)  | 0.2101 (6)  | 0.0489                                  |
| C(24) | 0.7599 (8)  | 0.0101 (6)  | 0.2336 (7)  | 0.0581                                  |
| C(25) | 0.8156 (7)  | 0.0534 (7)  | 0.2937 (7)  | 0.0578                                  |
| C(26) | 0.7441 (7)  | 0.1292 (6)  | 0.3281 (6)  | 0.0553                                  |
| C(27) | 0.5995 (7)  | 0.3036 (7)  | 0.3897 (7)  | 0.0580                                  |
| C(31) | 0.3062 (6)  | 0.3319 (5)  | 0.4220 (4)  | 0.0345                                  |
| C(32) | 0.2225 (6)  | 0.4144 (5)  | 0.4411 (5)  | 0.0407                                  |
| C(33) | 0.1810 (7)  | 0.4112 (6)  | 0.5347 (5)  | 0.0470                                  |
| C(34) | 0.2170 (7)  | 0.3243 (6)  | 0.6115 (5)  | 0.0446                                  |
| C(35) | 0.2929 (7)  | 0.2383 (6)  | 0.5948 (5)  | 0.0488                                  |
| C(36) | 0.3356 (6)  | 0.2413 (5)  | 0.5021 (5)  | 0.0406                                  |
| C(41) | 0.1240 (5)  | 0.2492 (5)  | 0.2869 (5)  | 0.0333                                  |
| C(42) | 0.1275 (7)  | 0.1528 (5)  | 0.3567 (6)  | 0.0453                                  |
| C(43) | 0.0571 (7)  | 0.1399 (6)  | 0.4411 (6)  | 0.0548                                  |
| C(44) | -0.0218 (6) | 0.2237 (6)  | 0.4557 (5)  | 0.0467                                  |
| C(45) | -0.0296 (7) | 0.3199 (6)  | 0.3881 (5)  | 0.0468                                  |
| C(46) | 0.0426 (6)  | 0.3341 (5)  | 0.3046 (5)  | 0.0422                                  |
| C(51) | 0.1470 (9)  | 0.6916 (8)  | 0.2322 (8)  | 0.0711                                  |
| C(52) | 0.582 (1)   | 0.5686 (9)  | 0.147 (1)   | 0.0850                                  |
| C(53) | 0.477 (1)   | 0.6147 (8)  | 0.3836 (8)  | 0.0710                                  |
| C(54) | 0.438 (1)   | 0.1586 (8)  | -0.0211 (7) | 0.0823                                  |
| C(55) | 0.373 (1)   | -0.0987 (8) | 0.293 (1)   | 0.0961                                  |
| C(56) | 0.140 (2)   | 0.004 (1)   | 0.092 (2)   | 0.1415                                  |

<sup>a</sup> *U*<sub>eq</sub> = one-third of the trace of the orthogonalized *U*<sub>*ij*</sub> tensor.

electrode) experiment reveals that 3<sup>2+</sup> undergoes two one-electron oxidations to 3<sup>4+</sup> through 3<sup>3+</sup> and two one-electron reductions to 3 through 3<sup>+</sup>, as shown in Scheme I. All the redox processes are diffusion controlled (*i*/*v*<sup>1/2</sup> constant for scan rates of 50–500 mV s<sup>-1</sup>) and fully reversible (i.e. for an oxidation process, *i*<sub>red</sub>/*i*<sub>ox</sub> = 1 and vice versa, for all scan rates used).

CPE (controlled-potential electrolysis) experiments on **1** show that the [Pd<sub>2</sub>]<sup>2+</sup> system is produced only if the applied potential is above 0.5 V; in these conditions a solution containing 3<sup>4+</sup> is produced. This suggests that the formation of 3<sup>2+</sup> by chemical oxidation is a complex process involving intermediates in a higher oxidation state.

Stoichiometric oxidation of 3<sup>2+</sup> with [Cp<sub>2</sub>Fe]PF<sub>6</sub> in dichloromethane affords 3<sup>3+</sup> or 3<sup>4+</sup>, respectively. Similarly, stoichiometric reduction of 3<sup>2+</sup>, 3<sup>3+</sup>, or 3<sup>4+</sup> with [CoCp<sub>2</sub>] in dichloromethane leads to the neutral complex **3**, which can be extracted in toluene. Conproportionation of 3<sup>2+</sup> and **3** gives 3<sup>+</sup>, but we could not isolate it with satisfactory analytical results.

Table III. Bond Lengths (Å) and Angles (deg) for  $C_{34}H_{40}N_6O_{10}P_2Pd_2$ 

|                  |           |                  |           |                   |           |                   |           |
|------------------|-----------|------------------|-----------|-------------------|-----------|-------------------|-----------|
| Pd(1)-Pd(2)      | 3.803 (1) | Pd(2)-P(2)       | 2.213 (2) | O(3)-C(53)        | 1.45 (1)  | O(6)-C(56)        | 1.42 (1)  |
| Pd(1)-P(1)       | 2.216 (2) | Pd(2)-N(2)       | 2.089 (5) | C(1)-C(11)        | 1.465 (9) | C(2)-C(21)        | 1.48 (1)  |
| Pd(1)-N(1)       | 2.079 (5) | Pd(2)-N(4)       | 2.117 (5) | C(1)-C(17)        | 1.486 (9) | C(2)-C(27)        | 1.48 (1)  |
| Pd(1)-N(3)       | 2.122 (5) | Pd(2)-C(22)      | 2.020 (7) | C(11)-C(12)       | 1.406 (9) | C(21)-C(22)       | 1.40 (1)  |
| Pd(1)-C(12)      | 2.010 (7) | P(2)-O(4)        | 1.561 (7) | C(11)-C(16)       | 1.399 (9) | C(21)-C(26)       | 1.38 (1)  |
| P(1)-O(1)        | 1.574 (5) | P(2)-O(5)        | 1.569 (6) | C(12)-C(13)       | 1.41 (1)  | C(22)-C(23)       | 1.40 (1)  |
| P(1)-O(2)        | 1.578 (5) | P(2)-O(6)        | 1.551 (7) | C(13)-C(14)       | 1.39 (1)  | C(23)-C(24)       | 1.39 (1)  |
| P(1)-O(3)        | 1.587 (5) | N(2)-N(3)        | 1.412 (7) | C(14)-C(15)       | 1.38 (1)  | C(24)-C(25)       | 1.38 (1)  |
| N(1)-N(4)        | 1.397 (7) | N(2)-C(2)        | 1.286 (9) | C(15)-C(16)       | 1.38 (1)  | C(25)-C(26)       | 1.39 (1)  |
| N(1)-C(1)        | 1.294 (8) | N(4)-C(41)       | 1.358 (8) | C(31)-C(32)       | 1.423 (9) | C(41)-C(42)       | 1.406 (9) |
| N(3)-C(31)       | 1.346 (8) | N(6)-O(9)        | 1.23 (1)  | C(31)-C(36)       | 1.431 (9) | C(41)-C(46)       | 1.428 (9) |
| N(5)-O(7)        | 1.23 (1)  | N(6)-O(10)       | 1.25 (1)  | C(32)-C(33)       | 1.38 (1)  | C(42)-C(43)       | 1.38 (1)  |
| N(5)-O(8)        | 1.23 (1)  | N(6)-C(44)       | 1.43 (1)  | C(33)-C(34)       | 1.39 (1)  | C(43)-C(44)       | 1.39 (1)  |
| N(5)-C(34)       | 1.439 (9) | O(4)-C(54)       | 1.41 (1)  | C(34)-C(35)       | 1.41 (1)  | C(44)-C(45)       | 1.39 (1)  |
| O(1)-C(51)       | 1.42 (1)  | O(5)-C(55)       | 1.44 (2)  | C(35)-C(36)       | 1.37 (1)  | C(45)-C(46)       | 1.38 (1)  |
| O(2)-C(52)       | 1.43 (1)  |                  |           |                   |           |                   |           |
| N(1)-Pd(1)-P(1)  | 172.1 (2) | N(2)-Pd(2)-P(2)  | 173.5 (2) | C(11)-C(1)-N(1)   | 113.9 (6) | C(21)-C(2)-N(2)   | 114.2 (6) |
| N(3)-Pd(1)-P(1)  | 96.1 (2)  | N(4)-Pd(2)-P(2)  | 94.4 (1)  | C(17)-C(1)-N(1)   | 123.4 (6) | C(27)-C(2)-N(2)   | 124.0 (6) |
| N(3)-Pd(1)-N(1)  | 91.2 (2)  | N(4)-Pd(2)-N(2)  | 90.8 (2)  | C(17)-C(1)-C(11)  | 122.6 (6) | C(27)-C(2)-C(21)  | 121.8 (6) |
| C(12)-Pd(1)-P(1) | 93.1 (2)  | C(22)-Pd(2)-P(2) | 94.8 (2)  | C(12)-C(11)-C(1)  | 117.0 (5) | C(22)-C(21)-C(2)  | 117.1 (6) |
| C(12)-Pd(1)-N(1) | 80.0 (2)  | C(22)-Pd(2)-N(2) | 80.3 (3)  | C(16)-C(11)-C(1)  | 122.6 (6) | C(26)-C(21)-C(2)  | 121.3 (7) |
| C(12)-Pd(1)-N(3) | 169.1 (2) | C(22)-Pd(2)-N(4) | 170.6 (2) | C(16)-C(11)-C(12) | 120.5 (6) | C(26)-C(21)-C(22) | 121.5 (7) |
| O(1)-P(1)-Pd(1)  | 117.3 (2) | O(4)-P(2)-Pd(2)  | 119.5 (3) | C(11)-C(12)-Pd(1) | 112.5 (5) | C(21)-C(22)-Pd(2) | 112.2 (5) |
| O(2)-P(1)-Pd(1)  | 119.0 (2) | O(5)-P(2)-Pd(2)  | 118.2 (3) | C(13)-C(12)-Pd(1) | 129.9 (5) | C(23)-C(22)-Pd(2) | 130.9 (6) |
| O(2)-P(1)-O(1)   | 97.2 (3)  | O(5)-P(2)-O(4)   | 94.9 (4)  | C(13)-C(12)-C(11) | 117.5 (6) | C(23)-C(22)-C(21) | 116.8 (6) |
| O(3)-P(1)-Pd(1)  | 110.9 (2) | O(6)-P(2)-Pd(2)  | 111.0 (3) | C(14)-C(13)-C(12) | 121.2 (7) | C(24)-C(23)-C(22) | 121.2 (8) |
| O(3)-P(1)-O(1)   | 106.4 (3) | O(6)-P(2)-O(4)   | 107.0 (5) | C(15)-C(14)-C(13) | 120.2 (8) | C(25)-C(24)-C(23) | 121.2 (8) |
| O(3)-P(1)-O(2)   | 104.3 (3) | O(6)-P(2)-O(5)   | 104.2 (4) | C(16)-C(15)-C(14) | 119.8 (7) | C(26)-C(25)-C(24) | 118.4 (7) |
| N(4)-N(1)-Pd(1)  | 123.1 (4) | N(3)-N(2)-Pd(2)  | 123.3 (4) | C(15)-C(16)-C(11) | 120.8 (7) | C(25)-C(26)-C(21) | 120.8 (8) |
| C(1)-N(1)-Pd(1)  | 116.2 (4) | C(2)-N(2)-Pd(2)  | 116.1 (4) | C(32)-C(31)-N(3)  | 117.8 (6) | C(42)-C(41)-N(4)  | 118.9 (6) |
| C(1)-N(1)-N(4)   | 120.0 (5) | C(2)-N(2)-N(3)   | 120.3 (5) | C(36)-C(31)-N(3)  | 125.1 (6) | C(46)-C(41)-N(4)  | 123.3 (6) |
| N(2)-N(3)-Pd(1)  | 110.2 (4) | N(1)-N(4)-Pd(2)  | 108.7 (4) | C(36)-C(31)-C(32) | 117.1 (6) | C(46)-C(41)-C(42) | 117.9 (6) |
| C(31)-N(3)-Pd(1) | 130.5 (4) | C(41)-N(4)-Pd(2) | 118.2 (4) | C(33)-C(32)-C(31) | 121.4 (6) | C(43)-C(42)-C(41) | 121.8 (7) |
| C(31)-N(3)-N(2)  | 118.6 (5) | C(41)-N(4)-N(1)  | 114.5 (5) | C(34)-C(33)-C(32) | 119.7 (7) | C(44)-C(43)-C(42) | 118.9 (7) |
| O(8)-N(5)-O(7)   | 122.0 (7) | O(10)-N(6)-O(9)  | 122.1 (8) | C(33)-C(34)-N(5)  | 119.7 (7) | C(43)-C(44)-N(6)  | 118.9 (7) |
| C(34)-N(5)-O(7)  | 118.5 (7) | C(44)-N(6)-O(9)  | 118.4 (8) | C(35)-C(34)-N(5)  | 119.6 (7) | C(45)-C(44)-N(6)  | 119.8 (7) |
| C(34)-N(5)-O(8)  | 119.5 (8) | C(44)-N(6)-O(10) | 119.5 (8) | C(35)-C(34)-C(33) | 120.7 (6) | C(45)-C(44)-C(43) | 121.2 (7) |
| C(51)-O(1)-P(1)  | 123.5 (5) | C(54)-O(4)-P(2)  | 124.3 (6) | C(36)-C(35)-C(34) | 119.9 (6) | C(46)-C(45)-C(44) | 120.2 (7) |
| C(52)-O(2)-P(1)  | 118.5 (6) | C(55)-O(5)-P(2)  | 119.0 (6) | C(35)-C(36)-C(31) | 120.9 (6) | C(45)-C(46)-C(41) | 119.9 (6) |
| C(53)-O(3)-P(1)  | 120.7 (5) | C(56)-O(6)-P(2)  | 124.8 (9) |                   |           |                   |           |

Scheme I

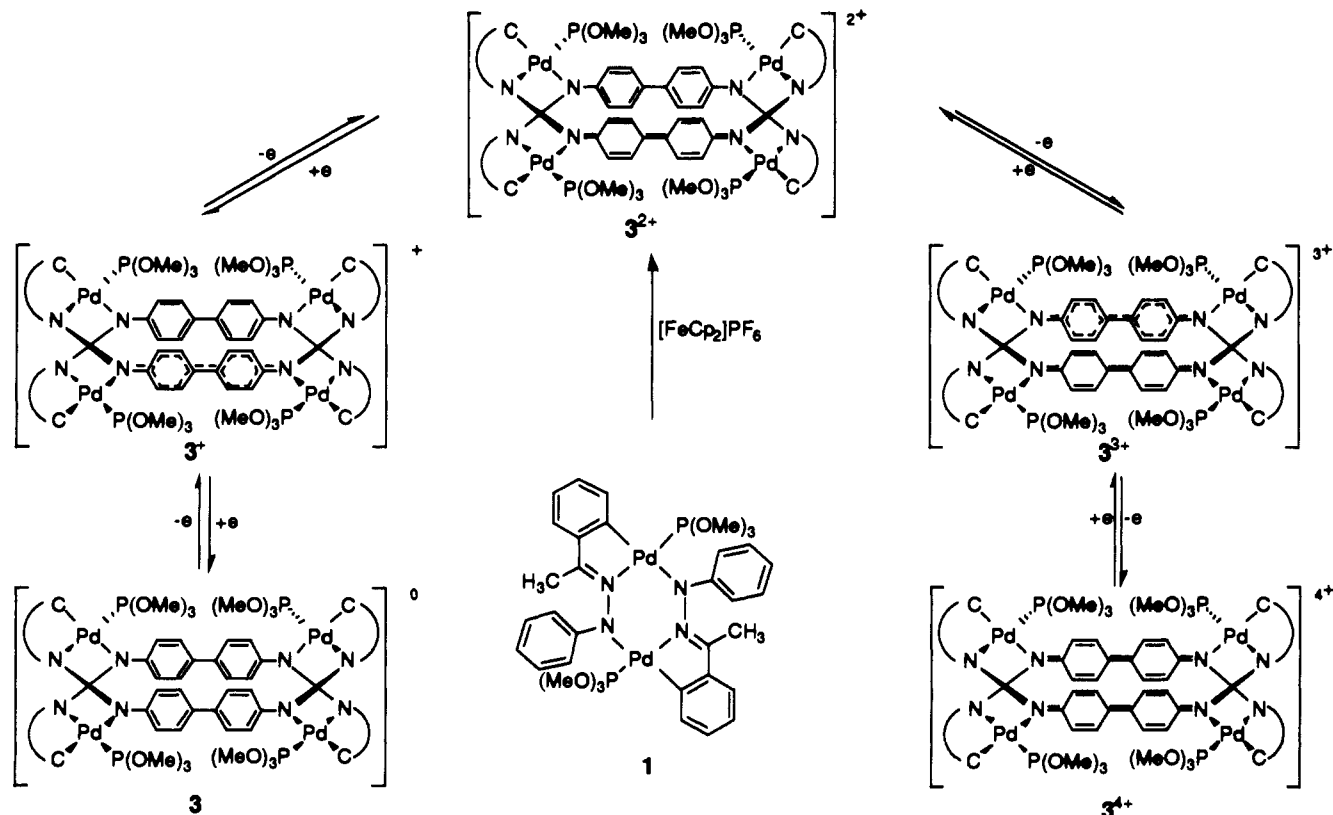


Table IV. CV Data for Compounds at a Platinum-Bead Electrode in CH<sub>2</sub>Cl<sub>2</sub><sup>a</sup>

| compd                               | 1                 | 2                 | 1a                | 2a                | L1                | L2                | any 3 <sup>2+</sup> | 7                 | 8                 |
|-------------------------------------|-------------------|-------------------|-------------------|-------------------|-------------------|-------------------|---------------------|-------------------|-------------------|
| E° <sub>1</sub> or E <sub>pk1</sub> | 0.04 <sup>i</sup> | 0.71 <sup>r</sup> | 0.03 <sup>i</sup> | 0.63 <sup>r</sup> | 1.02 <sup>i</sup> | 1.31 <sup>i</sup> | -0.51 <sup>r</sup>  | 1.35 <sup>i</sup> | 1.62 <sup>i</sup> |
| E° <sub>2</sub> or E <sub>pk2</sub> | 0.50 <sup>i</sup> | 1.09 <sup>r</sup> | 0.55 <sup>i</sup> | 1.08 <sup>r</sup> |                   |                   | -0.32 <sup>r</sup>  |                   |                   |
| E° <sub>3</sub>                     |                   |                   |                   |                   |                   |                   | 0.22 <sup>r</sup>   |                   |                   |
| E° <sub>4</sub>                     |                   |                   |                   |                   |                   |                   | 0.44 <sup>r</sup>   |                   |                   |
| ΔE <sub>1</sub>                     | 0.67              |                   | 0.60              |                   | 0.29              |                   |                     | 0.27              |                   |

<sup>a</sup>Supporting electrolyte is 0.1 M (TBA)PF<sub>6</sub>. Volts are referred to the saturated calomel electrode (SCE). Scan rates, 200 mV s<sup>-1</sup>. Superscript "i" refers to irreversible waves characterized by peak potentials E<sub>pk</sub>. Superscript "r" refers to reversible waves characterized by E° calculated as the average of the cathodic and anodic peak potentials.

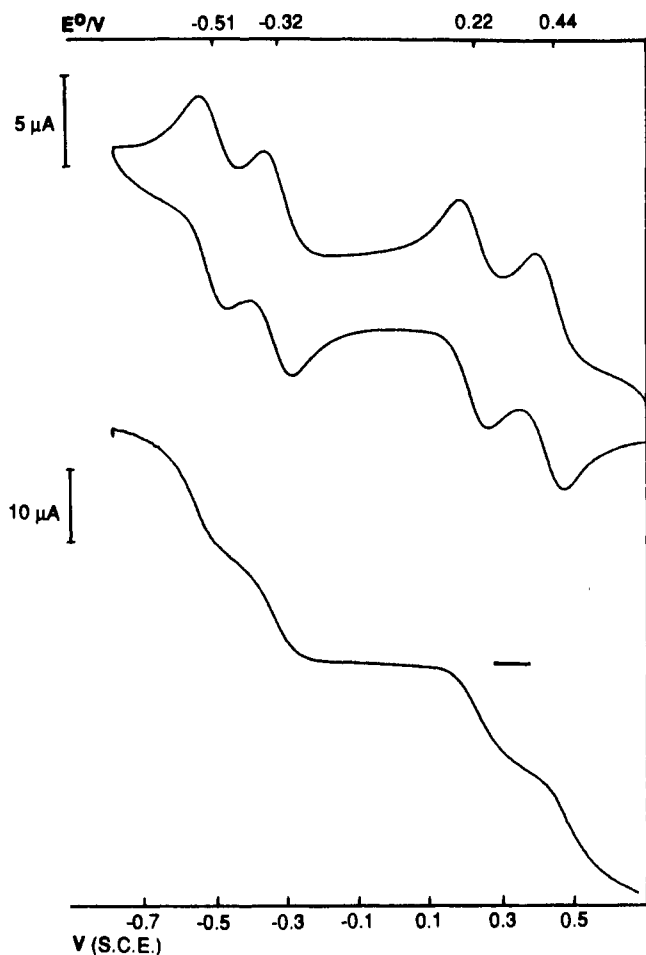


Figure 2. Cyclic voltammograms and rotating electrode curves of complex 3<sup>2+</sup> in CH<sub>2</sub>Cl<sub>2</sub>, 0.1 M (TBA)PF<sub>6</sub> at a Pt-bead electrode. Scan rate: (CV) 200 mV s<sup>-1</sup> and (RE) 20 mV s<sup>-1</sup>.

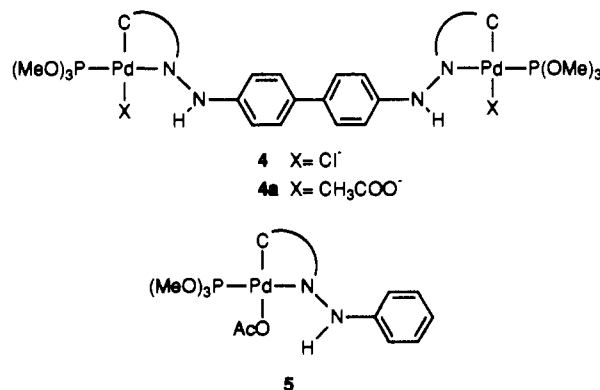
All attempts to grow suitable crystals of any 3<sup>n+</sup> for X-ray determination were unsuccessful. Although nice, apparently well-shaped, metallic-like bright-blue crystals of 3<sup>4+</sup> were obtained occasionally by diffusion or electrochemical methods,<sup>19</sup> in each occasion diffraction experiments proved them to be compact powders. However, the tetranuclear nature of the complexes is supported by mass spectrometry (FAB) of complex 3: A peak at *m/e* = 1750 with the expected pattern for the isotopic abundance of palladium was found. This is consistent with an oxidative coupling of two dimeric units of 1 involving the loss of one H<sub>2</sub> per dimer.

Magnetic measurements with a Gouy balance reveal diamagnetic behavior for 3, 3<sup>2+</sup>, and 3<sup>4+</sup>, whereas complex 3<sup>3+</sup> exhibits ESR response in a frozen glass (CH<sub>2</sub>Cl<sub>2</sub>-THF) at 105 K. The spectrum consists of a broad line with a *g* value of 1.997 (width 100 G, no hyperfine splitting observed).

3<sup>2+</sup> and 3<sup>4+</sup> show broad signals in their <sup>1</sup>H NMR spectra which remain unresolved and uninformative even at low temperature

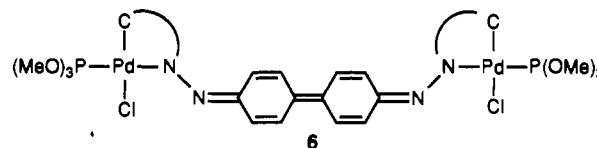
(-40 °C); we are not sure whether this broadening is due to unresolved nonrigid behavior of the complexes in solution or to traces of paramagnetic impurities below the level detectable in the Gouy balance. By contrast, clear <sup>1</sup>H and <sup>13</sup>C NMR spectra were obtained for complex 3. The <sup>1</sup>H NMR spectral data (given in the Experimental Section) support the proposed oxidative coupling. Further support is given by the <sup>13</sup>C and <sup>13</sup>C DEPT2 spectra, collected in Table V, which prove that C<sup>11</sup> has lost its hydrogen in complex 3.

Treatment of complex 3 with HCl or HAcO gives 4 or 4a as a result of bridge splitting by acidolysis of the Pd-N(amido) bonds. This behavior is similar to that reported<sup>5</sup> for the dimer 1, which



gives the corresponding monomer 5. Comparison of the <sup>13</sup>C NMR spectra (Table V) of 4a and 5 (and also of their <sup>1</sup>H NMR spectra; see Experimental Section) again reveals that 4a is the oxidative coupling product of 5 through the C<sup>11</sup> carbon atoms.

Treatment of 3<sup>4+</sup> with [(PhCH<sub>2</sub>)Et<sub>3</sub>N]Cl also produces bridge splitting, affording 6 where a quinone diimine ligand is trapped and stabilized between two palladium atoms. Reduction of 6 with



cobaltocene in nonaqueous media affords 3; it is remarkable that <sup>31</sup>P and <sup>1</sup>H NMR spectra show that, differently from the single product 3 obtained by reduction of 3<sup>2+</sup>, in this case 3 consists of a mixture of diastereomers. Thus, whereas 3 from 3<sup>2+</sup> shows only one <sup>31</sup>P resonance at 130.8 ppm and one <sup>1</sup>H doublet (P(OMe)<sub>3</sub>) at 3.33 ppm, 3 from 6 exhibits two <sup>31</sup>P resonances of similar intensity at 130.8 and 129.8 ppm and two very close but distinct <sup>1</sup>H doublets at 3.33 and 3.34 ppm.

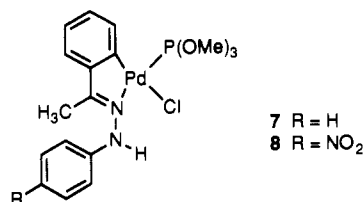
## Discussion

**Electrochemistry.** E<sub>pk</sub> values for 1 and 1a and E° values for 2 and 2a (Table IV) show that these potentials are scarcely altered by the replacement of P(OMe)<sub>3</sub> with 4-methylpyridine. Since both the metal atom and the five-membered moiety in the orthopalladated hydrazone should be quite sensitive to changes in the ancillary ligands, we conclude that the HOMO's in these complexes are little shared by the five-membered metallacycle.

A comparison of the first oxidation potential of the free ligands (acetophenone phenylhydrazone, L1; acetophenone (*p*-nitrophenyl)hydrazone, L2), their mononuclear orthopalladated com-

(19) Stephens, D. A.; Rehan, A. E.; Compton, S. J.; Barkhan, R. A.; Williams, J. M. *Inorg. Synth.* 1986, 24, 135.

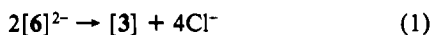
plexes (7 and 8), and the N,N'-bridged dimers (1,1a and 2,2a)



shows that oxidation of the latter is noticeably easier. This is to be expected since replacement of N-H by N-Pd on dimerization should increase the electron density on the ligand, more precisely near the position where this replacement has occurred. Replacement of H by NO<sub>2</sub> increases the oxidation potentials in the free ligands, the mononuclear complexes, and the binuclear complexes, but this increase is higher in the latter (see  $\Delta E_1$  values in Table IV); in other words the electron-withdrawing ability of the NO<sub>2</sub> substituent attenuates the effect produced by Pd in the dimers, as is to be expected. All these data suggest that the HOMO electron removed in the oxidation process is mainly based on the R-C<sub>6</sub>H<sub>4</sub>-N part of the molecule.

From the electrochemical data in Table IV conproportionation constants for the processes  $3^{(n+1)+} + 3^{(n-1)+} \rightleftharpoons 3^{n+}$  can be calculated ( $K_c = 10^{\Delta E/0.059}$ ). The  $K_c$  values for  $3^+$  ( $1.7 \times 10^3$ ),  $3^{2+}$  ( $1.4 \times 10^9$ ), and  $3^{3+}$  ( $1.9 \times 10^4$ ) show that these complexes are stable toward disproportionation. Thus, benzidine diamido ligands turn promising as bridging ligands capable of stabilizing mixed oxidation states of a molecule, which is a goal of current research,<sup>20-22</sup> and in the design of molecules of interest as photoreductors in photochemical electron-transfer processes.<sup>23,24</sup>

The cyclic voltammogram of complex 6 is shown in Figure 3. Scanning from +0.75 to -0.45 V (a in Figure 3) gives a flat voltammogram (i.e. no waves are present). Further scanning to more negative potentials (b in Figure 3) produces an irreversible wave at -0.6 V; in the reverse scan small anodic waves appear at -0.28, +0.26, and +0.45 V. The irreversible reduction at -0.6 V is assigned to the two-electron process  $6/6^{2-}$ . At this point, two units of  $6^{2-}$  undergo coupling according to eq 1.



In the reverse scan 3 shows oxidations to  $3^+$ ,  $3^{2+}$ ,  $3^{3+}$ , and  $3^{4+}$ , but  $3^{4+}$  is able to react with the Cl<sup>-</sup> liberated in the coupling step, giving back 6. In consequence, the intensities of the cathodic waves due to reductions of  $3^{4+}$  depend on the scan rate, as expected for a chemical step (reaction with Cl<sup>-</sup>) following the electron transfer. In (b) of Figure 3 the scan rate is 100 mV s<sup>-1</sup> and cathodic peaks are not seen, but in (c) where the scan rate was 200 mV s<sup>-1</sup> these peaks begin to be observed. At scan rates of 1700 mV s<sup>-1</sup> the CV shown in Figure 4 is obtained: The reduction of 6 appears now as two peaks (two electrons are involved) and the  $3^{4+}/3^{3+}$  and  $3^{3+}/3^{2+}$  electron transfers have become reversible, meaning that the chemical reaction of  $3^{4+}$  with Cl<sup>-</sup> has been suppressed.

The cyclic voltammograms shown in Figure 5 were recorded on a solution obtained by controlled-potential electrolysis of 6 at -0.75 V: A scanning from -0.75 to -0.15 V shows reversible waves for the processes  $3/3^+$  and  $3^+/3^{2+}$ ; however, if the potential +0.55 V is reached, formation of 6 (by reaction in the electrode of  $3^{4+}$  with chloride) occurs, being noticeable by the increased intensity of the cathodic wave at -0.6 V in the reverse scan.

**UV-Vis-NIR Spectra.** All complexes of the  $3^{n+}$  series show a strong absorption in the range 400-500 nm with  $\epsilon$  values about 50 000 M<sup>-1</sup> cm<sup>-1</sup>, which can be assigned to MLCT or LMCT transitions. Compounds  $3^{2+}$  and  $3^{3+}$  show an additional band near

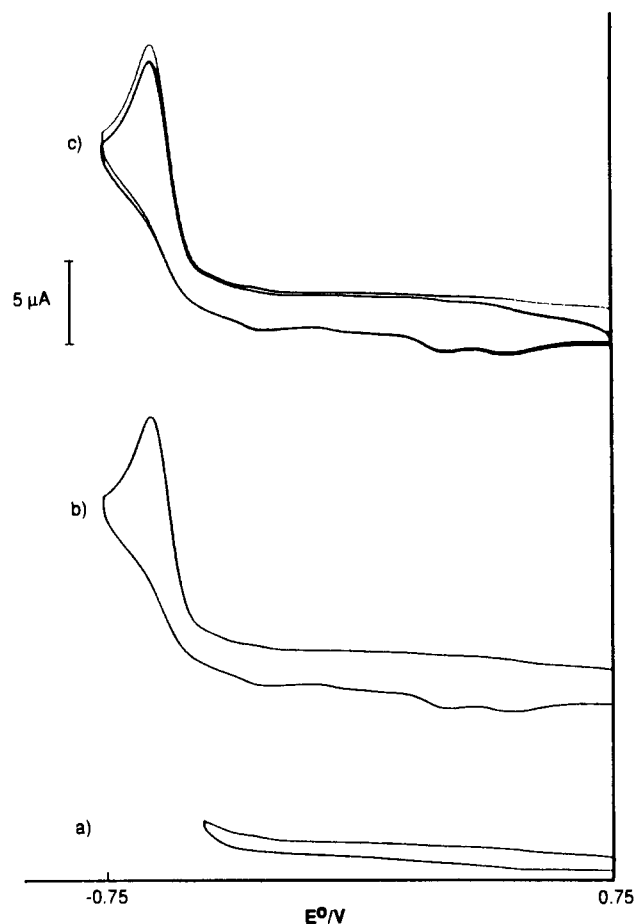


Figure 3. Cyclic voltammograms of complex 6 in CH<sub>2</sub>Cl<sub>2</sub>, 0.1 M (TBA)PF<sub>6</sub> at a Pt-bead electrode. Scan rates: 100 mV s<sup>-1</sup> in (a) and (b) and 200 mV s<sup>-1</sup> in (c).

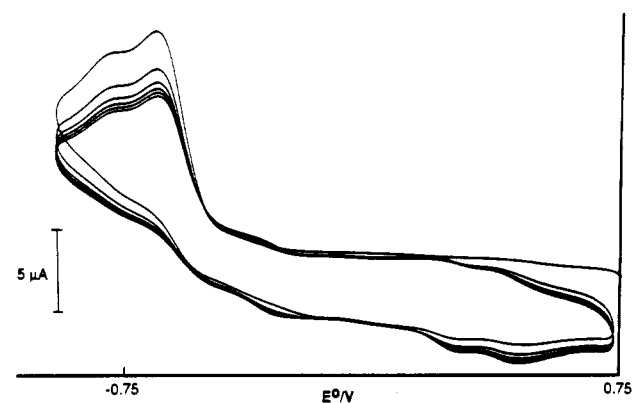


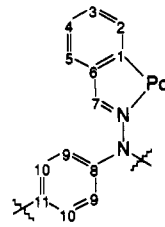
Figure 4. Cyclic voltammograms of complex 6 in CH<sub>2</sub>Cl<sub>2</sub>, 0.1 M (TBA)PF<sub>6</sub> at a Pt-bead electrode. Scan rate: 1700 mV s<sup>-1</sup>.

800 nm, which is tentatively assigned to an intraligand transition in the semiquinone bridge present in these complexes by analogy with the assignment made for semiquinone-type cation radicals of tetramethylbenzidine.<sup>25</sup> Complex  $3^{3+}$  can be seen as a species in a mixed oxidation state; if all palladium atoms are considered to be Pd(II) one bridge is the quinone diimine type and the other semiquinone diimine. The observed bands in the NIR region for  $3^{3+}$ , with *maxima* at 1250 and 1500 nm, can be assigned to typical IT bands for mixed oxidation states.

**Stereochemical Aspects.** Complex 1 is chiral and is obtained<sup>5</sup> as a racemic mixture; consequently, the coupling reactions can lead to meso or rac diastereomers for 3 (Figure 6). 3 prepared by reduction of 6 contains a 1:1 mixture of the two possible

- (20) Ernst, S.; Kasack, V.; Kaim, W. *Inorg. Chem.* **1988**, *27*, 1146.  
 (21) Kaim, W.; Kasack, V. *Inorg. Chem.* **1990**, *29*, 4696.  
 (22) Richardson, D. E.; Taube, H. *J. Am. Chem. Soc.* **1983**, *105*, 40.  
 (23) Benbouazza, A.; Buntinx, G.; Poizat, O.; Valat, P.; Wintgens, V. *New J. Chem.* **1990**, *14*, 629.  
 (24) Guichard, V.; Bourkba, A.; Poizat, O.; Buntinx, G. *J. Phys. Chem.* **1989**, *93*, 4429.

- (25) Alkatis, S. A.; Grätzel, M. *J. Am. Chem. Soc.* **1976**, *98*, 3549.

Table V. Relevant  $^{13}\text{C}$  NMR Data for Complexes 3, 4a, and 5 (at 75.47 MHz,  $\delta$  ppm, referenced to TMS)


| carbon | complex (solvent)            |   |                                     |                                     |                                     |                                     |
|--------|------------------------------|---|-------------------------------------|-------------------------------------|-------------------------------------|-------------------------------------|
|        | 3 ( $\text{C}_6\text{D}_6$ ) | 3 <sup>a</sup> ( $\text{CD}_2\text{Cl}_2$ ) | 4a ( $\text{CDCl}_3$ )              | 4a <sup>a</sup> ( $\text{CDCl}_3$ ) | 5 ( $\text{CDCl}_3$ )               | 5 <sup>a</sup> ( $\text{CDCl}_3$ )  |
| 1      | 180.9                        |   | 183.6                               |                                     | 183.4 ( $^2J_{\text{C-P}} = 3$ Hz)  |                                     |
| 2      | 137.8                        | 137.6 ( $^3J_{\text{C-P}} = 6$ Hz)          | 137.0 ( $^3J_{\text{C-P}} = 11$ Hz) | 137.0 ( $^3J_{\text{C-P}} = 11$ Hz) | 137.0 ( $^3J_{\text{C-P}} = 11$ Hz) | 137.0 ( $^3J_{\text{C-P}} = 11$ Hz) |
| 3      | <i>b</i>                     | 128.6 ( $^4J_{\text{C-P}} = 6$ Hz)          | 131.1 ( $^4J_{\text{C-P}} = 6$ Hz)  | 131.1 ( $^4J_{\text{C-P}} = 6$ Hz)  | 131.1 ( $^4J_{\text{C-P}} = 6$ Hz)  | 131.1 ( $^4J_{\text{C-P}} = 6$ Hz)  |
| 4      | <i>b</i>                     | 128.3                                       | 124.9                               | 124.9                               | 124.9                               | 124.9                               |
| 5      | 126.8                        | 126.6                                       | 128.0                               | 128.0                               | 128.0                               | 128.0                               |
| 6      | 152.9                        |   | 144.3                               |                                     | 145.5                               |                                     |
| 7      | 162.1                        |   | 153.4                               |                                     | 153.4                               |                                     |
| 8      | 149.3                        |   | 145.9                               |                                     | 145.9                               |                                     |
| 9      | 124.8                        | 124.8                                       | 114.7                               | 114.7                               | 114.4                               | 114.4                               |
| 10     | 126.8                        | 126.7                                       | 127.5                               | 127.5                               | 129.2                               | 129.2                               |
| 11     | 129.3                        |   | 134.3                               |                                     | 121.5                               | 121.5                               |
| 12     |                              |   | 177.9 <sup>c</sup>                  |                                     | 177.7 <sup>c</sup>                  |                                     |

<sup>a</sup>DEPT2 data. <sup>b</sup>Benzene signals preclude observation. <sup>c</sup>12 refers to the carboxylic acetate carbon when present.

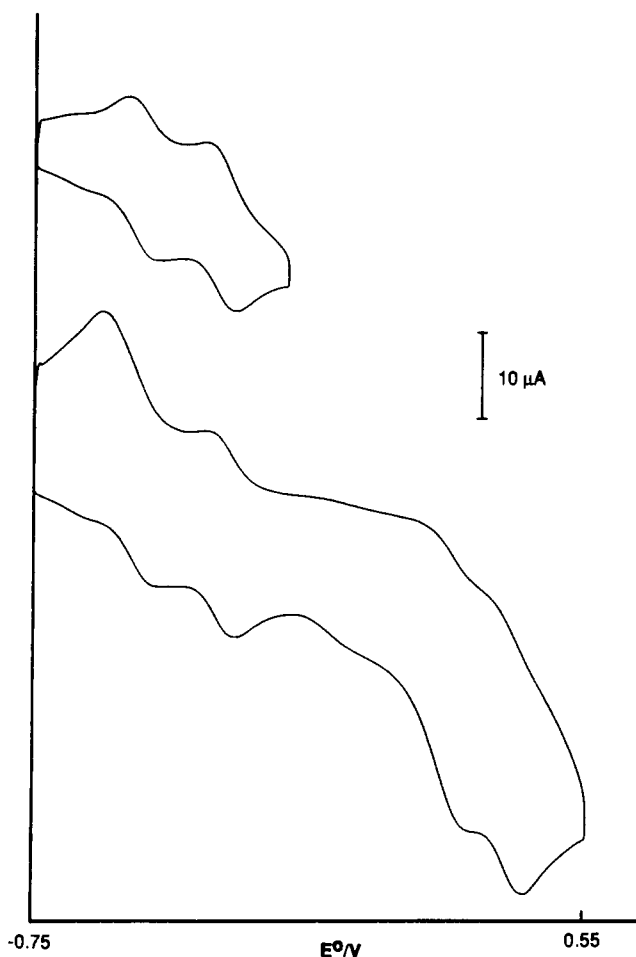


Figure 5. Cyclic voltammograms after controlled-potential electrolysis at  $-0.9$  V of complex 6 in  $\text{CH}_2\text{Cl}_2$ ,  $0.1$  M (TBA) $\text{PF}_6$ . Scan rate:  $200$   $\text{mV s}^{-1}$ .

isomers. However, 3 prepared by oxidative coupling of 1 contains only one diastereomer (as X-ray determination was not possible, we are unable to assign it to meso or rac). Hence the electrochemical synthesis follows, with asymmetric induction arising

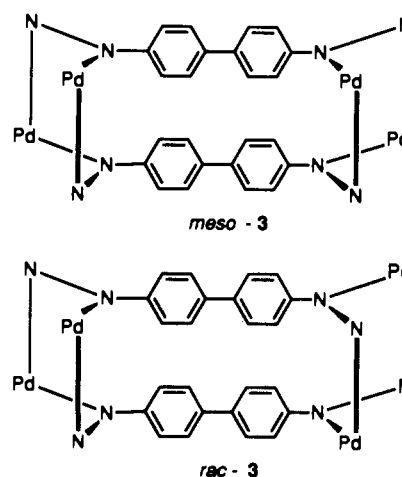


Figure 6. Meso and rac isomers for complex 3.

probably from restrictions (not obvious from models) to the coupling combination that should have produced the diastereomer not formed (this aborted coupling would follow with decomposition, hence the low yield in the reaction).

**Acknowledgment.** We thank Dr. Neil G. Connely (Bristol U.K.) for suggestions and mass spectrometry measurements, Dr. Miguel A. Ruiz (Oviedo, Spain) for NMR measurements, The Dirección General de Investigación Científica y Técnica (Project PB89-0360) and the Caja de Ahorros Municipal de Burgos for financial support.

**Registry No.** 1, 123264-64-2; 1a, 123264-62-0; 2, 123264-64-2; 2a, 141248-29-5; meso-3, 141248-25-1; rac-3, 141317-21-7; 3<sup>+</sup>, 141248-34-2; 3<sup>2+</sup>, 141248-31-9; 3<sup>3+</sup>, 141248-33-1; 3<sup>4+</sup>, 141248-32-0; 4, 141248-26-2; 4a, 141248-30-8; 5, 123264-66-4; 6, 141248-27-3; 7, 123264-57-3; 8, 141248-28-4;  $[\text{FeCp}_2]\text{PF}_6$ , 11077-24-0;  $\text{CoCp}_2$ , 1277-43-6.

**Supplementary Material Available:** Tables of positional and thermal parameters of H atoms and anisotropic thermal parameters (3 pages); structure factor tables (18 pages). Ordering information is given on any current masthead page. Full crystallographic data have been deposited at the Cambridge Crystallographic Data Centre.